1836 *Chem. Mater.* **2010,** *22,* 1836–1845
DOI:10.1021/cm903542v

CHEMISTRY OF MATERIALS
Article

D-π-A Sensitizers for Dye-Sensitized Solar Cells: Linear vs Branched Oligothiophenes

Markus K. R. Fischer,[†,§] Sophie Wenger,[‡,§] Mingkui Wang,[‡] Amaresh Mishra,*[,†] Shaik M. Zakeeruddin,*[,‡] Michael Grätzel,*[,‡] and Peter Bäuerle*[,†]

[†]*Institute of Organic Chemistry II and Advanced Materials, University of Ulm, Albert-Einstein-Allee 11, D-89081 Ulm, Germany, and* [‡]*Laboratory of Photonics and Interfaces, Institute of Chemical Sciences and Engineering, Ecole Polytechnique Fédérale de Lausanne (EPFL), Station 6, CH-1015 Lausanne, Switzerland.* [§] *These authors contributed equally to this work.*

Received November 23, 2009. Revised Manuscript Received January 11, 2010

Two donor-π-acceptor (D-π-A) dyes, coded as L-3T-DPA **1** and B-5T-DPA **2**, were synthesized for application in dye-sensitized solar cells. These D-π-A sensitizers use diphenylamine as donor, an oligothiophene as π-bridge, and cyanoacrylic acid as an acceptor group that can be anchored to the surface of TiO_2. While the two dyes comprise the same donor and acceptor units, the bridging oligothiophene is linear in one case and branched in the other case. Photophysical and electrochemical properties of the dyes were investigated by UV−vis spectrometry and cyclic voltammetry. The dyes were subsequently implemented as sensitizers in dye-sensitized solar cells. Photovoltaic devices with dye **1** showed a maximum monochromatic incident photon to current efficiency (IPCE) of 80% and an overall conversion efficiency of 6.8% under full sunlight (AM 1.5G, 100 mW cm^{-2}) irradiation. The photovoltaic performance of branched dye **2** was lower because of less dye loading on the TiO_2 surface. The dyes were also tested in ionic liquid and solid-state devices and showed good efficiencies. Long-term stability measurements were performed over 1000 h at full sunlight and at 60 °C in ionic liquid devices. Branched dye **2** thereby showed excellent stability retaining 96% of its initial efficiency, while linear dye **1** retained 73% after 1000 h of irradiation.

Introduction

The conversion of solar energy to electricity is attracting considerable attention as a form of clean renewable energy resources. In this context, dye-sensitized solar cells (DSSCs) are considered as a credible alternative to conventional inorganic silicon-based solar cells.[1,2] Compared to silicon solar cells, DSSCs offer major advantages such as low material cost, tunability of the absorption spectrum, and encouraging efficiency even under diffuse light. DSSCs efficiently convert solar energy into electricity using either Ru^{II}-polypyridyl complexes or metal-free organic dyes, and efficiencies over 11% have been reported using ruthenium sensitizers.[1,3,4] In recent years, metal-free organic dyes have attracted increased interest as an alternative to ruthenium complexes because of low material costs, ease of synthesis, high molar extinction coefficients, and environmental friendly materials.[5] Although remarkable advances have been made with metal-free organic dyes as sensitizers in DSSCs and efficiencies exceeding 9% have been reached, there is still a need to optimize their chemical and physical properties for further improvement of the device performance.[6,7]

The properties of D-π-A dyes can be easily tuned by varying donor, spacer, and acceptor moieties. Our intention was to use electron rich oligothiophenes as π-conjugated bridge as they are known to be ideal building blocks for DSSCs.[5,8] Upon photoexcitation, electron transfer from the donor to the acceptor is a fast process

*Corresponding author: amaresh.mishra@uni-ulm.de (A.M.), peter.baeuerle@uni-ulm.de (P.B.), shaik.zakeer@epfl.ch (S.M.K.), michael.graetzel@epfl.ch (M.G.).

(1) (a) Grätzel, M. *Nature* **2001**, *414*, 338. (b) O'Regan, B.; Grätzel, M. *Nature* **1991**, *353*, 737.
(2) (a) Hagfeldt, A.; Grätzel, M. *Acc. Chem. Res.* **2000**, *33*, 269. (b) Grätzel, M. *Acc. Chem. Res.* **2009**, *42*, 1788. (c) Yanagida, S.; Yu, Y.; Manseki, K. *Acc. Chem. Res.* **2009**, *42*, 1827.
(3) Nazeeruddin, M. K.; Pechy, P.; Renouard, T.; Zakeeruddin, S. M.; Humphry-Baker, R.; Comte, P.; Liska, P.; Cevey, L.; Costa, E.; Shklover, V.; Spiccia, L.; Deacon, G. B.; Bignozzi, C. A.; Grätzel, M. *J. Am. Chem. Soc.* **2001**, *123*, 1613.
(4) (a) Chiba, Y.; Islam, A.; Watanabe, Y.; Komiya, R.; Koide, N.; Han, L. *Jpn. J. Appl. Phys.* **2006**, *45*, L638. (b) Cao, Y.; Bai, Y.; Yu, Q.; Cheng, Y.; Liu, S.; Shi, D.; Gao, F.; Wang, P. *J. Phys. Chem. C* **2009**, *113*, 6290. (c) Gao, F.; Wang, Y.; Shi, D.; Zhang, J.; Wang, M.; Jing, X.; Humphry-Baker, R.; Wang, P.; Zakeeruddin, S. M.; Grätzel, M. *J. Am. Chem. Soc.* **2008**, *130*, 10720. (d) Cao, Y.; Bai, Y.; Yu, Q.; Cheng, Y.; Liu, S.; Shi, D.; Gao, F.; Wang, P. *J. Phys. Chem. C* **2009**, *113*, 6290. (e) Chen, C.-Y.; Wang, M.; Li, J.-Y.; Pootrakulchote, N.; Alibabaei, L.; Ngoc-le, C.-h.; Decoppet, J.-D.; Tsai, J.-H.; Grätzel, C.; Wu, C.-G.; Zakeeruddin, S. M.; Grätzel, M. *ACS Nano* **2009**, *3*, 3103.
(5) Mishra, A.; Fischer, M. K. R.; Bäuerle, P. *Angew. Chem., Int. Ed.* **2009**, *48*, 2474.
(6) (a) Ferrere, S.; Zaban, A.; Gregg, B. A. *J. Phys. Chem. B* **1997**, *101*, 4490. (b) Tian, H.; Liu, P.-H.; Zhu, W.; Gao, E.; Wu, D.-J.; Cai, S. *J. Mater. Chem.* **2000**, *10*, 2708. (c) Ferrere, S.; Gregg, B. A. *New J. Chem.* **2002**, *26*, 1155.
(7) (a) Ito, S.; Zakeeruddin, S. M.; Humphry-Baker, R.; Liska, P.; Charvet, R.; Comte, P.; Nazeeruddin, M. K.; Péchy, P.; Takata, M.; Miura, H.; Uchida, S.; Grätzel, M. *Adv. Mater.* **2006**, *18*, 1202. (b) Zhang, G.; Bala, H.; Cheng, Y.; Shi, D.; Lv, X.; Yu, Q.; Wang, P. *Chem. Commun.* **2009**, 2198.
(8) Ooyama, Y.; Harima, Y. *Eur. J. Org. Chem.* **2009**, 2903.

 Published on Web 01/27/2010

to generate charge-separated species. In this respect, triphenylamine or substituted derivatives have been successfully used as donors for sensitizers in dye-sensitized solar cells.[9,10] It has also been observed that the structure of the π-conjugated bridging group played a decisive role in device performance.[11] The bridging group can serve both, as a part of the light absorbing chromophore and as a pathway for transporting charges. Herein, we present synthesis and characterization of a linear and a related branched dye comprising diphenylamine oligothiophene and cyanoacrylic acid. These dyes were charecterized in DSSCs using volatile solvent-based electrolyte, ionic liquid electrolyte, and a solid organic hole-conductor (spiro-MeOTAD) as redox mediator.

Experimental Section

General Remarks. NMR spectra were recorded on a Bruker AMX 500 (^{1}H NMR: 500 MHz, ^{13}C NMR: 125 MHz) or an Avance 400 spectrometer (^{1}H NMR: 400 MHz, ^{13}C NMR: 100 MHz), normally at 25 °C. Chemical shift values (δ) are expressed in parts per million using residual solvent protons (^{1}H NMR, δ_H = 7.26 for $CDCl_3$ and δ_H = 3.57 for THF-d_8; ^{13}C NMR, δ_C = 77.0 for $CDCl_3$ and δ_C = 67.2 for THF-d_8) as internal standard. The splitting patterns are designated as follows: s (singlet), d (doublet), t (triplet), m (multiplet), and q (quartet). The assignments are PhH (phenyl protons), CHO (aldehyde proton), and ThH (thiophene protons). Melting points were determined using a Büchi B-545 apparatus and were not corrected. Elemental analyses were performed on an Elementar Vario EL. Thin layer chromatography was carried out on aluminum plates, precoated with silica gel, Merck Si60 F_{254}. Preparative column chromatography was performed on glass columns packed with silica gel, Merck Silica 60, particle size 40-43 μm. CI mass spectra were recorded on a Finnigan MAT SSQ-7000, EI-mass were recorded on a Varian Saturn 2000 GC-MS, and MALDI-TOF mass spectra on a Bruker Daltonics Reflex III.

Materials. Tetrahydrofurane (Merck) was dried under reflux over sodium/benzophenone (Merck). Dimethylformamide (Merck) was first refluxed over P_4O_{10} (Merck) and distilled, then refluxed over BaO (Riedel-de Haën), and distilled again. The dry dimethylformamide was stored over molar sieve (4 Å). All synthetic steps were carried out under argon atmosphere (except Knoevenagel condensation). 2-Isopropoxy-4,4,5,5-tetramethyl-1,3,2-dioxaborolane was purchased from Aldrich and was dried over molar sieve (4 Å) prior to use, $Pd_2(dba)_3 \cdot CHCl_3$, $HP(^tBu)_3BF_4$, *n*-BuLi (1.6 mol L^{-1} in hexane) were purchased from Acros, diphenylamine and NaO^tBu were purchased from Fluka, cyanoacetic acid was purchased from ABCR, and ammonium acetate was purchased from Merck. The potassium phosphate solution was prepared by dissolving potassium phosphate monohydrate (Riedel-de Haën) in deionized water and was degassed prior to use.

5-Bromo-3′,4′-diethyl-2,2′:5′,2″-terthiophene (4). To a solution of terthiophene **3** (1.0 g, 3.29 mmol) in dry dimethylformamide (30 mL) was added dropwise at 0 °C *N*-bromosuccinimide (585 mg, 3.29 mmol, dissolved in 30 mL of dry dimethylformamide). The reaction mixture was allowed to warm to room temperature and was stirred for another 3 h. The reaction mixture was poured into water and extracted three times with diethyl ether. The combined organic extracts were washed with water (5 × 200 mL), brine (2 × 100 mL), filtered, and dried over Na_2SO_4. The solvent was removed by rotary evaporation. After column chromatography (SiO_2, hexane) terthiophene **4** (880 mg, 2.3 mmol, 70%) was obtained as a colorless viscous oil. ^{1}H NMR ($CDCl_3$, 400 MHz) δ ppm: 1.22 (t, ^3J = 7.55 Hz, 3H, CH_3), 1.22 (t, ^3J = 7.55 Hz, 3H, CH_3), 2.73 (q, ^3J = 7.56 Hz, 2H, CH_2), 2.75 (q, ^3J = 7.56 Hz, 2H, CH_2), 6.89 (d, ^3J = 3.86 Hz, 1H), 7.02 (d, ^3J = 3.86 Hz, 1H), 7.07 (dd, ^3J = 5.16, 3.60 Hz, 1H), 7.15 (dd, ^3J = 3.60, ^4J = 1.15 Hz, 1H), 7.32 (dd, ^3J = 5.16, ^4J = 1.15 Hz, 1H). ^{13}C NMR ($CDCl_3$, 100 MHz) δ ppm: 15.29, 15.37, 20.99, 21.03, 111.78, 125.53, 126.06, 126.11, 127.40, 128.80, 130.19, 130.39, 135.77, 137.60, 141.13, 141.64. EI-mass 382 [M^+] (calcd. for $C_{16}H_{15}BrS_3$ 381.95). Elemental analysis: calc. (%) for $C_{16}H_{15}BrS_3$ C: 50.12; H: 3.94; S: 25.09; found: C: 50.19; H: 3.96; S: 25.04.

***N,N*-Diphenyl-3′,4′-diethyl-2,2′:5′,2″-terthiophene-5-amine (5).** 5-Bromoterthiophene **4** (500 mg, 1.3 mmol, 1.0 equiv), diphenylamine (220 mg, 1.3 mmol, 1.0 equiv), and NaO^tBu (138 mg, 1.44 mmol, 1.1 equiv) were added to a Schlenk tube. Then dry degassed toluene (10 mL) was added to the mixture. $Pd_2(dba)_3 \cdot CHCl_3$ (13.5 mg, 13 μmol, 0.01 equiv) and $HP(t\text{Bu})_3BF_4$ (7.6 mg, 26.1 μmol, 0.02 equiv) were suspended in 2 mL of dry degassed toluene and stirred for 10 min. The catalyst suspension was then added to the reactants. The reaction mixture was stirred for 12 h at 100 °C. The solvent was subsequently removed under reduced pressure. The mixture was redissolved in dichloromethane, and the resulting solution was washed with water and brine and dried over Na_2SO_4. After column chromatography (SiO_2, hexane:DCM = 3:1) amine **5** (505 mg, 1.07 mmol, 82%) was obtained as a slightly yellow semisolid. ^{1}H NMR ($CDCl_3$, 400 MHz) δ ppm: 1.22 (t, ^3J = 7.53 Hz, 3H, CH_3), 1.22 (t, ^3J = 7.53 Hz, 3H, CH_3), 2.76 (q, ^3J = 7.52 Hz, 2H, CH_2), 2.77 (q, ^3J = 7.52 Hz, 2H, CH_2), 6.65 (d, ^3J = 3.87 Hz, 1H, ThH), 6.94 (d, ^3J = 3.88 Hz, 1H, ThH), 7.02−7.10 (m, 3H, PhH + ThH), 7.15 (dd, ^3J = 3.59, ^4J = 1.12 Hz, 1H, ThH), 7.18−7.22 (m, 4H, PhH), 7.26−7.32 (m, 5H, PhH + ThH). ^{13}C NMR ($CDCl_3$, 100 MHz) δ ppm: 15.31, 15.33, 20.99, 21.09, 121.15, 122.59, 123.06, 124.18, 125.20, 125.70, 127.36, 129.17, 129.28, 130.20, 130.36, 136.13, 140.60, 141.10, 147.65, 151.11. EI-mass 472 [M+H]$^+$ (calcd. for $C_{28}H_{25}NS_3$ 471.11). Elemental analysis: calc. (%) for $C_{28}H_{25}NS_3$ C: 71.30; H: 5.34; N: 2.97; found: C: 71.34; H: 5.33; N: 2.86.

5-Diphenylamino-3′,4′-diethyl-2,2′:5′,2″-terthiophene-5″-carbaldehyde (6). *n*-BuLi (0.44 mL, 0.70 mmol, 1.6 mol L^{-1}, 1.1 equiv) was added dropwise at −78 °C to a solution of **5** (300 mg, 0.64 mmol, 1.0 equiv) in 5 mL of dry THF, and the mixture was kept at this temperature and stirred for 0.5 h. Dry dimethylformamide (92 μL, 1.27 mmol, 2.0 equiv) was added. The reaction mixture was allowed to warm to room temperature and stirred for another

(9) (a) Velusamy, M.; JustinThomas, K. R.; Lin, J. T.; Hsu, Y. C.; Ho, K. C. *Org. Lett.* **2005**, *7*, 1899. (b) Hagberg, D. P.; Edvinsson, T.; Marinado, T.; Boschloo, G.; Hagfeldt, A.; Sun, L. *Chem. Commun.* **2006**, 2245. (c) Justin Thomas, K. R.; Hsu, Y.-C.; Lin, J. T.; Lee, K.-M.; Ho, K.-C.; Lai, C.-H.; Cheng, Y.-M.; Chou, P.-T. *Chem. Mater.* **2008**, *20*, 1830. (d) Ning, Z.; Tian, H. *Chem. Commun.* **2009**, 5483.

(10) (a) Bonhote, P.; Moser, J.-E.; Humphry-Baker, R.; Vlachopoulos, N.; Zakeeruddin, S. M.; Walder, L.; Grätzel, M. *J. Am. Chem. Soc.* **1999**, *121*, 1324. (b) Hagberg, D. P.; Marinado, T.; Karlsson, K. M.; Nonomura, K.; Qin, P.; Boschloo, G.; Brinck, T.; Hagfeldt, A.; Sun, L. *J. Org. Chem.* **2007**, *72*, 9550. (c) Qin, P.; Zhu, H.; Edvinsson, T.; Boschloo, G.; Hagfeldt, A.; Sun, L. *J. Am. Chem. Soc.* **2008**, *130*, 8570. (d) Qin, H.; Wenger, S.; Xu, M.; Gao, F.; Jing, X.; Wang, P.; Zakeeruddin, S. M.; Grätzel, M. *J. Am. Chem. Soc.* **2008**, *130*, 9202. (e) Tian, H.; Yang, X.; Chen, R.; Zhang, R.; Hagfeldt, A.; Sun, L. *J. Phys. Chem. C* **2008**, *112*, 11023. (f) Ning, Z.; Zhang, Q.; Wu, W.; Pei, H.; Liu, B.; Tian, H. *J. Org. Chem.* **2008**, *73*, 3791. (g) Choi, H.; Baik, C.; Kang, S. O.; Ko, J.; Kang, M.-S.; Nazeeruddin, M. K.; Grätzel, M. *Angew. Chem., Int. Ed.* **2008**, *47*, 327.

(11) Wang, Z.-S.; Koumura, N.; Cui, Y.; Takahashi, M.; Sekiguchi, H.; Mori, A.; Kubo, T.; Furube, A.; Hara, K. *Chem. Mater.* **2008**, *20*, 3993.

2 h. HCl (3 mL, 6 mol L^{-1}) was added for hydrolysis, and the mixture was stirred for 0.5 h. The mixture was neutralized with a $NaHCO_3$-solution and extracted with diethyl ether (3 × 20 mL). The combined organic phases were washed with water and brine and dried over Na_2SO_4. The solvent was removed by rotary evaporation, and the residue was purified by column chromatography (SiO_2, hexane:dichloromethane = 1:2) to provide carbaldehyde **6** (248 mg, 0.50 mmol, 78%) as a red oil. ^{1}H NMR ($CDCl_3$, 400 MHz) δ ppm: 1.22 (t, ^3J = 7.50 Hz, 3H, CH_3), 1.25 (t, ^3J = 7.50 Hz, 3H, CH_3), 2.76 (q, ^3J = 7.50 Hz, 2H, CH_2), 2.84 (q, ^3J = 7.50 Hz, 2H, CH_2), 6.64 (d, ^3J = 3.88 Hz, 1H, ThH), 6.97 (d, ^3J = 3.92 Hz, 1H, ThH), 7.03−7.10 (m, 2H, PhH), 7.15−7.23 (m, 4H, PhH), 7.23 (d, ^3J = 4.08 Hz, 1H, ThH), 7.27−7.32 (m, 4H, PhH), 7.69 (d, ^3J = 3.99 Hz, 1H, ThH), 9.87, (s, 1H, CHO). ^{13}C NMR ($CDCl_3$, 100 MHz) δ ppm: 14.82, 15.21, 20.99, 21.26, 120.55, 122.75, 123.28, 124.84, 125.72, 128.04, 128.82, 129.19, 132.83, 136.88, 141.03, 141.81, 143.57, 146.33, 147.47, 152.04, 182.55. CI-mass 499.9 $[M+H]^+$ (calcd. for $C_{29}H_{25}NOS_3$ 499.11) Elemental analysis: calc. (%) for $C_{29}H_{25}NOS_3$ C: 69.70; H: 5.04; N: 2.80; found: C: 69.84; H: 5.23; N: 2.67.

2-Cyano-3-[5-diphenylamino-3′,4′-diethyl-2,2′:5′,2″-terthien-5″-yl]acrylic Acid (1). A mixture of carbaldehyde **6** (200 mg, 0.4 mmol, 1.0 equiv) and cyanoacetic acid (102 mg, 1.2 mmol, 3 equiv) was vacuum-dried, and acetonitrile (20 mL) was added together with piperidine (16 μL, 0.2 mmol). The mixture was refluxed for 6 h. After cooling, the solvent was removed in vacuum. The residue was then dissolved in dichloromethane and washed with water and brine and finally dried over Na_2SO_4. The solvent was removed by rotary evaporation, and the crude product was purified by column chromatography (SiO_2, dichloromethane:methanol = 3:1) to provide dye **1** (165 mg, 0.29 mmol, 73%) as a red solid. Mp: 245−247 °C. ^{1}H NMR ($CDCl_3$, 500 MHz) δ ppm: 1.10 (t, ^3J = 7.43, 3H), 1.12 (t, ^3J = 7.43, 3H), 2.67 (q, ^3J = 7.54 Hz, 2H), 2.73 (d, ^3J = 7.54 Hz, 2H), 6.55 (d, ^3J = 3.90 Hz, 1H, ThH), 6.89 (d, ^3J = 3.87 Hz, 1H, ThH), 6.96−7.01 (m, 2H, PhH), 7.08 (d, ^3J = 3.77 Hz, 1H, ThH), 7.10−7.14 (m, 4H, PhH), 7.19−7.24 (m, 4H, PhH), 7.61 (d, ^3J = 3.95 Hz, 1H, ThH), 8.34 (s, 1H, C=CH). ^{13}C NMR ($CDCl_3$, 125 MHz) δ ppm: 14.22, 14.52, 20.66, 20.94, 117.66, 120.64, 122.59, 123.06, 124.63, 125.47, 125.77, 128.68, 128.99, 129.22, 131.96, 136.05, 140.70, 142.53, 142.89, 147.66, 151.77, 164.01. CI-mass 567.1 $[M+H]^+$ (calcd. for $C_{32}H_{26}N_2O_2S_3$ 566.12). Elemental analysis: calc. (%) for $C_{32}H_{26}N_2O_2S_3$ C: 67.81; H: 4.62; N: 4.94; found: C: 67.69; H: 4.65; N: 4.85.

***N,N*-Diphenylthiophene-2-amine (7).** The compound was prepared according to the literature procedure.[12,13] 2-Bromothiophene (489 mg, 3.0 mmol, 1.0 equiv), diphenylamine (508 mg, 3.0 mmol, 1.0 equiv), and NaO*t*Bu (317 mg, 3.3 mmol, 1.1 equiv) were weighed into a round-bottom flask, and dry degassed toluene (3 mL) was added. $Pd_2(dba)_3\cdot CHCl_3$ (31.1 mg, 30 μmol, 0.01 equiv) and $HP(tBu)_3BF_4$ (17.4 mg, 60 μmol, 0.02 equiv) were suspended in 3 mL of dry degassed toluene and stirred for 10 min. The catalyst suspension was added to the reactants to give a purple reaction mixture. The reaction was stirred for 16 h at 105 °C. The solvent was removed under reduced pressure. The product (415 mg, 1.7 mmol, 55%) was obtained after column chromatography (neutral alumina, hexane) as a colorless solid. The analytical data were the same as in the literature.

***N,N*-Diphenyl-5-(4,4,5,5-tetramethyl-1,3,2-dioxaborolan-2-yl)-thiophene-2-amine (8).** A THF (15 mL) solution of *N*,*N*-diphenylthiophene-2-amine **7** (1.50 g, 5.97 mmol, 1.0 equiv) was cooled to −78 °C. *n*-BuLi (4.48 mL, 7.16 mmol, 1.60 mol L^{-1}, 1.2 equiv) was added dropwise to the above solution and stirred for 0.5 h while keeping the temperature at around −78 °C. 2-Isopropyloxy-4,4,5,5-tetramethyl-1,3,2-dioxaborolane (1.39 g, 7.46 mmol, 1.25 equiv) was added dropwise at −78 °C. The reaction mixture was allowed to warm to room temperature and was stirred for 1 h. The reaction was quenched with a saturated NH_4Cl-solution (50 mL) and extracted three times with 50 mL of diethyl ether. The combined organic extracts were washed with brine and dried over Na_2SO_4. The solvent was removed after filtration under reduced pressure. Boronic ester **8** (2.42 g, 5.96 mmol, 100%, 93% GC-purity) was obtained as a greenish viscous oil, which solidified upon cooling and was used for further reactions without any purification. ^{1}H NMR ($CDCl_3$, 400 MHz) δ ppm: 1.32 (s, CH_3), 6.66 (d, ^3J = 3.74 Hz, 1H), 7.03−7.09 (m, 2H, PhH), 7.15−7.20 (m, 4H, PhH), 7.24−7.29 (m, 4H, PhH), 7.41 (d, ^3J = 3.75 Hz, 1H). ^{13}C NMR ($CDCl_3$, 100 MHz) δ ppm: 24.73, 83.82, 118.86, 122.29, 123.59, 123.66, 129.08, 129.24, 136.80, 147.70, 159.07. EI-mass (*m*/*z*) 378 $[M+H]^+$, 377 ($[M^+]$ (calcd. for $C_{22}H_{24}BNO_2S$ 377.16).

***N,N,N‴,N‴*-Tetraphenyl-2,2′:5′,2″:3″,2‴:5‴,2⁗-quinquethiophene-5,5⁗-diamine (10).** Branched terthiophene **9** (0.500 g, 1.0 mmol, 1.0 equiv), boronic ester **8** (0.830 g, 2.2 mmol, 2.2 equiv), $Pd_2(dba)_3\cdot CHCl_3$ (21 mg, 0.02 mmol, 0.02 equiv), and $HP(tBu)_3BF_4$ (12 mg, 0.04 mmol, 0.04 equiv) were dissolved in 15 mL of well-degassed THF. A well-degassed aqueous K_3PO_4 solution (6.0 mL, 6.0 mmol, 1 mol L^{-1}, 6.0 equiv) was added slowly. The reaction mixture was stirred at room temperature for 5 h. Water (20 mL) with a few drops of HCl (2 mol L^{-1}) was added to the mixture. The organic layer was separated, and the aqueous layer was extracted three times with 10 mL of diethyl ether/ethyl acetate (1:1). The combined organic extracts were washed with brine and dried over Na_2SO_4. The solvents were removed under reduced pressure, and the residue was purified by column chromatography (crude product on silica gel, hexane:EtOAc = 19:1). The resulting precleaned product was finally purified by preparative HPLC (hexane:DCM = 80:20) to provide diamine **10** (0.225 g, 3.01 mmol, 75%) as a yellow-orange solid. Mp 79 °C. ^{1}H NMR ([D_8] THF, 400 MHz) δ ppm: 6.57 (d, ^3J = 3.90 Hz, 2H, ThH), 6.96 (d, ^3J = 3.90 Hz, 1H, ThH) 6.98−7.04 (m, 9H, PhH + ThH), 7.11−7.14 (m, 8H, PhH + ThH), 7.19 (d, ^3J = 5.30 Hz, 1H, ThH), 7.22−7.26 (m, 8H, PhH + ThH), 7.43 (d, ^3J = 5.30 Hz, 1H, ThH). ^{13}C NMR ([D_8] THF, 100 MHz) δ ppm: 121.8, 122.1, 122.9, 123.3, 123.4, 123.4, 123.6, 123.6, 123.8, 123.9, 126.0, 128.1, 129.5, 129.8, 129.8, 130.3, 131.4, 131.5, 132.0, 132.7, 133.5, 136.3, 138.6, 139.9, 148.4, 148.5, 151.4, 151.8. MS (MALDI-TOF): *m*/*z* 745.9 $[M]^+$ (calc. for $C_{44}H_{30}N_2S_5$: 746.1). Elemental analysis: calc. (%) for $C_{44}H_{30}N_2S_5$ C: 70.74; H: 4.05; N: 3.75; found: C: 70.92; H: 4.05; N: 3.64.

5,5⁗-Bis(diphenylamino)-2,2′:5′,2″:3″,2‴:5‴,2⁗-quinquethiophene-5″-carbaldehyde (11). *N*-BuLi (0.19 mL, 0.30 mmol, 1.6 mol L^{-1}, 1.5 equiv) was added dropwise at −78 °C to a solution of diamine **10** (150.0 mg, 0.20 mmol, 1.0 equiv) in 5 mL of dry THF, and the mixture was stirred for 0.5 h at this temperature. Dry dimethylformamide (94 μL, 1.20 mmol, 6.0 equiv) was added dropwise via syringe. The reaction mixture was allowed to warm to room temperature. Then HCl (3 mL, 6 mol L^{-1}) was added for hydrolysis, and the mixture was stirred for 0.5 h. The mixture was neutralized with a $NaHCO_3$-solution and then extracted with diethyl ether (3 × 20 mL). The combined organic phases were washed with brine and dried over Na_2SO_4. The solvent was removed by rotary evaporation, and the residue was purified by column chromatography (compound on silica, hexane:dichloromethane = 1:1) to provide carbaldehyde **11** as a red oil. The pro-

(12) Watanabe, M.; Yamamoto, T.; Nishiyama, M. *Chem. Commun.* **2000**, 133.
(13) Hooper, M. W.; Utsunomiya, M.; Hartwig, J. F. *J. Org. Chem.* **2003**, *68*, 2861.

duct was redissolved in a small amount of THF and precipitated into methanol. After concentration under reduced pressure and filtration, the product (111 mg, 0.14 mmol, 74%) was obtained as a red powder. Mp 85 °C. ^{1}H NMR ([D$_8$] THF, 400 MHz) δ ppm: 6.56 (d, ^3J = 3.92 Hz, 1H, ThH), 6.58 (d, ^3J = 3.89 Hz, 1H, ThH), 6.99−7.06 (m, 8H, PhH), 7.09 (d, ^3J = 3.76 Hz, 1H, ThH), 7.11−7.15 (m, 8H, PhH + ThH), 7.22−7.27 (m, 9H, PhH + ThH), 7.90 (s, 1H ThH), 9.84 (s, 1H, CHO). ^{13}C NMR ([D$_8$] THF, 100 MHz) δ ppm: 121.3, 121.8, 123.3, 123.4, 123.5, 123.6, 123.7, 123.9, 124.1, 124.1, 129.4, 129.8, 129.8, 130.3, 130.5, 131.3, 132.2, 132.6, 134.4, 139.4, 139.7, 141.0, 141.5, 142.1, 148.3, 148.4, 151.8, 152.6, 182.6. MS (MALDI-TOF): m/z 774.2 [M]$^+$ (calc. for $C_{45}H_{30}N_2OS_5$: 774.1). Elemental analysis: calc. (%) for $C_{45}H_{30}N_2OS_5$ C: 69.73; H: 3.90; N: 3.61; found: C: 69.60; H: 3.96; N: 3.59.

2-Cyano-3-[5,5′′′′-bis(diphenylamino)-2,2′:5′,2′′:3′′,2′′′:5′′′,2′′′′-quinquethien-5′′-yl]acrylic Acid (2). Aldehyde **11** (50.0 mg, 64.5 μmol, 1.0 equiv), cyanoacetic acid (16.5 mg, 194 μmol, 3.0 equiv), and ammonium acetate (2.49 mg, 32.3 μmol, 0.5 equiv) were suspended in glacial acetic acid (5 mL) and stirred under reflux for 5 h. The mixture was cooled and extracted three times with dichloromethane. The organic phase was washed with a $NaHCO_3$-solution and then with brine and finally dried over Na_2SO_4. The solvent was removed after filtration by rotary evaporation, and the residue was purified by column chromatography (silica, dichloromethane, and 5% glacial acetic acid) to provide **2** as a dark red solid. The solid was redissolved in 2 mL of tetrahydrofurane and precipitated into 15 mL of methanol under vigorous stirring. The precipitate was sonicated for 1 h, filtered off, and washed with a large amount water and subsequently with methanol (50 mL). After drying under high vacuum product **2** (43.0 mg, 51.1 μmol, 79%) was obtained as a dark red solid. Mp: 249 °C. ^{1}H NMR ([D$_8$]THF, 500 MHz) δ ppm: 6.48−6.60 (m, 2H, ThH), 6.90−7.07 (m, 9H, PhH + ThH), 7.09−7.17 (m, 8H, PhH + ThH), 7.20−7.30 (m, 9H, PhH + ThH), 7.83 (s, 1H, ThH), 8.32 (s, 1H, C = CH). ^{13}C NMR ([D$_8$]THF, 125 MHz) δ ppm: 100.5, 117.1, 121.2, 121.8, 123.3, 123.4, 123.4, 123.6, 123.8, 123.9, 124.1, 129.5, 129.8, 129.8, 130.5, 130.5, 131.3, 131.4, 131.4, 132.1, 132.2, 132.3, 141.6, 145.5, 148.3, 148.4, 148.4, 148.4, 163.9. MS (MALDI-TOF): m/z 841.5 [M]$^+$ (calc. for $C_{48}H_{31}N_3O_2S_5$: 841.1). Elemental analysis: calc. (%) for $C_{48}H_{31}N_3O_2S_5$ C: 68.46; H: 3.71; N: 4.99; found: C: 68.17; H: 3.90; N: 4.75.

Optical and Voltammetric Measurements. Optical measurements were carried out in 1 cm cuvettes with Merck Uvasol grade solvents, and absorption spectra were recorded on a Perkin-Elmer Lambda 19 spectrometer. Cyclic voltammetry experiments were performed with a computer-controlled EG&G PAR 273 potentiostat in a three-electrode single-compartment cell with a platinum working electrode, a platinum wire counter electrode, and an Ag/AgCl reference electrode. All potentials were internally referenced to the ferrocene/ferrocenium couple. The concentration of molecules adsorbed on the TiO_2 film ("dye loading") was calculated using the Lambert−Beer law and the molar extinction coefficient of the dye in solution.

Device Fabrication. Dyes were tested in photovoltaic devices using standard mesoporous TiO_2 films with a 8 μm thick transparent layer of 20 nm sized particles and a 5 μm thick scattering layer of 400 nm sized particles on top of fluorine-doped tin oxide (FTO) coated glass. The detailed fabrication procedures for the TiO_2 pastes and film have been described elsewhere.[14] Films were immersed for 5 h in a solution of 0.3 mM dye and 10 mM chenodeoxycholic acid (cheno) as coadsorbant in dichloromethane. Cells were sealed with a platinized FTO counter electrode using a hot-melt (Surlyn, DuPont). Cells were then filled with an electrolyte through a hole in the counter electrode. The hole was then sealed with a Surlyn disk and a thin glass to avoid leakage of the electrolyte. We compared the photovoltaic performance using a volatile solvent-based electrolyte (coded as Z960) and an ionic liquid electrolyte (coded as Z952). The composition of the electrolytes was as follows: Z960: 1.0 M 1,3-dimethylimidazolium iodide, 0.03 M iodine, 0.1 M guanidinium thiocyanate, 0.5 M tert-butylpyridine, 0.05 M LiI in a mixture of acetonitrile and valeronitrile (85/15, v/v). Z952: 1,3-dimethylimidazoliumiodide/1-ethyl-3-methylimidazoliumiodide/1-ethyl-3methylimidazolium tetracyanoborate/iodine/N-butylbenzoimidazole/guanidinium thiocyanate (molar ratio 12/12/16/1.67/3.33/0.67). The photoanode was covered with a UV-cutoff/antireflecting polymer.

For solid-state device fabrication, a spray pyrolysis technique was used to coat the FTO conducting glass substrates (LOF Industries, TEC 15 Ω/square, 2.2 mm thickness) with a thin compact layer of TiO_2 in order to prevent electron−hole recombination arising from direct contact between the hole-conductor (spiro-OMeTAD) and the highly doped FTO layer. A 1.8 μm mesoporous layer of the TiO_2 nanoparticles with a typical diameter of 20 nm was deposited by doctor-blading on top of this compact layer. The TiO_2 electrodes were stained by dipping in a dye solution for 5 h consisting of 0.3 mM dye and 10 mM cheno in dichloromethane. The spiro-OMeTAD solution (137 mM in chlorobenzene) contained final concentrations of 112 mM tert-butylpyridine and 21 mM Li[CF_3SO_2]$_2$N (added from highly concentrated acetonitrile solutions). Finally, a gold contact (100 nm) was deposited on the organic semiconductor film by evaporation (EDWARDS AUTO 500 Magnetron Sputtering System).

Photovoltaic Characterization and Stability Tests. A 450 W xenon light source (Oriel, USA) was used to give an irradiance of 100 mW cm^{-2} (the equivalent of one sun at air mass global, AM 1.5G, at the surface of solar cells). The spectral output of the lamp was matched in the region of 350−750 nm with the aid of a Schott K113 Tempax sunlight filter (Präzisions Glas & Optik GmbH, Germany) to reduce the mismatch between the simulated and true solar spectra to less than 2%. The current−voltage characteristics of the cells were obtained by applying an external potential bias to the cell and measuring the generated photocurrent with a Keithley model 2400 digital source meter (Keithley, USA). The effective area of the devices was defined with the use of a metal mask to be 0.159 cm^2.

A similar data acquisition system was used to control the incident photon-to-current conversion efficiency (IPCE) measurement. Under computer control, light from a 300 W xenon lamp (ILC Technology, USA) was focused through a Gemini-180 double monochromator (Jobin Yvon Ltd., UK) onto the photovoltaic cell under test. A computer-controlled monochromator was incremented through the spectral range (300−900 nm) to generate a photocurrent action spectrum with a sampling interval of 10 nm and a current sampling time of 5 s. For stability tests, devices were irradiated at open-circuit under a Suntest CPS plus lamp (ATLAS GmBH, 100 mW cm^{-2}) in ambient air at 60 °C.

Transient Photovoltage and Photocurrent Decay Measurements. Transient decays were measured with different white light steady-state biases and a superimposed red light perturbation pulse (0.05 s square pulse width, 100 ns rise and fall time), incident on the photoanode side of the test device. The white and red lights were supplied by light-emitting diodes. The voltage

(14) Wang, P.; Zakeeruddin, S. M.; Comte, P.; Charvet, R.; Humphry-Baker, R.; Grätzel, M. *J. Phys. Chem. B* **2003**, *107*, 14336.

Scheme 1. Synthesis of Dye 1[a]

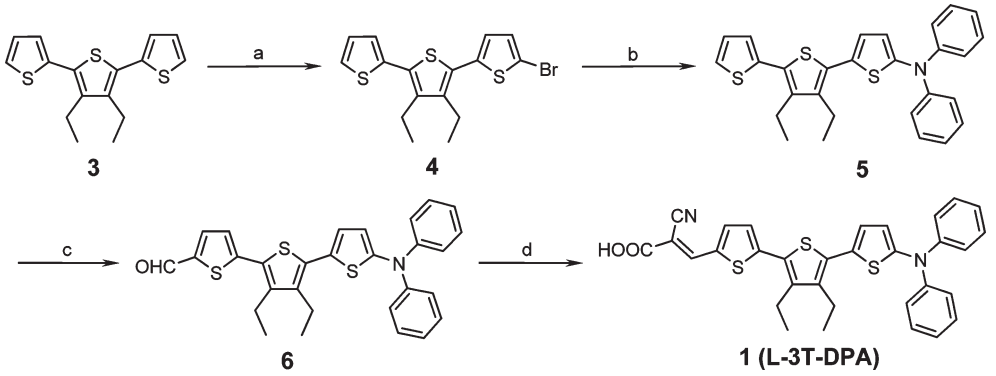

[a] a) NBS, DMF, 0 °C to RT, 70%. b) Diphenylamine, $[Pd_2(dba)_3]\cdot CHCl_3$, $HP(tBu)_3BF_4$, NaO*t*Bu, toluene, 100 °C, 82%. c) 1. *n*-BuLi, −78 °C, THF, 1 h, 2. DMF, 2 h, 3. HCl, 78%. d) Cyanoacetic acid, piperidine, acetonitrile, 80 °C, 4 h, 73%.

Scheme 2. Synthesis of Dye 2[a]

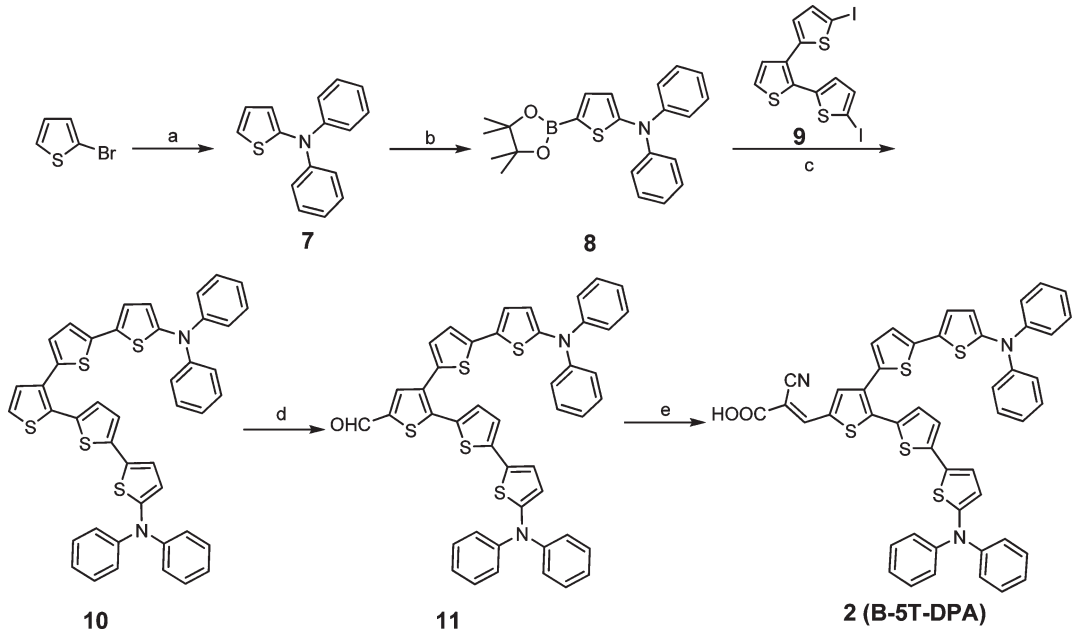

[a] a) 1. $[Pd_2(dba)_3]\cdot CHCl_3$, $HP(^tBu)_3BF_4$, NaO^{t}Bu, toluene, 16 h, 105 °C, 55%. b) 1. *n*-BuLi, −78 °C, THF, 1 h, 2. 2-Isopropyloxy-4,4,5,5-tetramethyl-1,3,2-dioxaborolane, 1 h, 93%. c) $[Pd_2(dba)_3]\cdot CHCl_3$, $HP(^tBu)_3BF_4$, THF, 5 h, 25 °C. d) 1. *n*-BuLi, −78 °C, THF, 1 h, 2. DMF, 2 h, 3. HCl, 74%. e) Cyanoacetic acid, NH_4OAc, glacial acetic acid, reflux, 5 h, 79%.

dynamics were recorded at open-circuit on a PC-interfaced Keithley 2400 source meter with a 500 μs response time. The perturbation light source was set to a suitably low level for the voltage decay kinetics to be monoexponential. By varying the white light bias intensity, the recombination rate constant could be estimated at open-circuit potentials of the device (corresponding to different free charge densities in the TiO_2 film). The chemical capacitance (C) at the TiO_2/electrolyte interface was calculated from the amount of injected charge by the red pulse (ΔQ) and the associated increase in photovoltage (ΔV) using $C = \Delta Q/\Delta V$. The injected charge was obtained from integration of the short-circuit photocurrent transient. The density of trap states (DOS) was calculated from DOS $= C/[ed(1\text{-}p)]$, where e is the elementary charge, C is the capacitance in F cm^{-2}, d is the film thickness, and p is the porosity of the film (68%).

Results and Discussion

Synthesis. Linear and branched dyes L-3T-DPA **1** and B-5T-DPA **2** were synthesized as follows (Schemes 1 and 2). Monobromination of terthiophene **3** using *N*-bromosuccinimide in dimethylformamide afforded bromoterthiophene **4** in 70% yield (Scheme 1). Cross-coupling of 5-bromoterthiophene **4** and diphenylamine by Pd-catalyzed Hartwig-Buchwald reaction[12,13] gave amine **5** in 82% yield. Deprotonation of the free α-position of **5** using *n*-butyl lithium (*n*-BuLi) and subsequent reaction of the lithium species with dimethylformamide furnished corresponding aldehyde **6** in 78% yield. Finally, linear dye **1** was prepared in 73% yield by a Knoevenagel condensation of aldehyde **6** with cyanoacetic acid using piperidine as catalyst.

Branched dye **2** was synthesized starting from 2-bromothiophene and diphenylamine, which were converted to *N,N*-diphenyl-thiophene-2-amine **7** via a Hartwig-Buchwald reaction. Deprotonation of the free α-position at the thiophene ring of **7** with *n*-BuLi and subsequent reaction with 2-isopropoxy-4,4,5,5-tetramethyl-1,3,2-dioxaborolane as electrophile afforded boronic ester **8** in 93% yield (Scheme 2). A 2-fold Suzuki-type cross-coupling reaction of branched diiodinated terthiophene

9[15] with boronic ester **8** gave peripheral-functionalized dendritic oligothiophene **10** in 75% yield. Aldehyde **11** was prepared in 74% yield by lithiation of **10** at the core and quenching of the metalated species with anhydrous dimethylformamide. Knoevenagel condensation of aldehyde **11** and cyanoacetic acid under acidic conditions furnished corresponding dye **2** in 79% yield.

Photophysical Properties. Absorption and emission spectra of the two dyes in dichloromethane solution are displayed in Figure 1, and the corresponding data are presented in Table 1. Dye **1** showed an absorption maximum in the visible region at 450 nm with a molar extinction coefficient of 19600 M^{-1} cm^{-1}, arising from a charge transfer (CT) transition. On the other hand, dye **2** showed a CT transition at 503 nm, which compared to dye **1** is 53 nm red-shifted but somewhat weaker (16600 M^{-1} cm^{-1}). The molar extinction coefficients of the transitions at higher energy (390 nm, 300 nm) are approximately doubled for branched dye **2** compared to linear dye **1** (386 nm, 295 nm). The shape of the absorption spectra of **1** and **2** are comparable to similar dyes where the thiophenes adjacent to the diphenylamine moieties are replaced by phenyl rings.[9c] Emission maxima of dyes **1** and **2** can be found at 694 and 791 nm, respectively, when excited at their respective CT bands. A large Stoke's shift was observed for both dyes **1** (7813 cm^{-1}) and **2** (7238 cm^{-1}), which is an indication of significant structural changes between the ground and the excited state and, accordingly, specify a photoinduced charge transfer process.

A negative solvatochromism was observed for the charge transfer band by increasing polarity of the solvent (Figure 2a,b), indicating that the dyes possess smaller dipole moments in the excited state than in the ground state. This is due to the fact that in polar solvents the electron-withdrawing power of the carboxylic acid decreases because of its partial deprotonation in the excited state. This information was further supported by the blue-shift (about 20 nm) of the CT band upon addition of triethylamine to dye solutions in THF or 1,4-dioxane. A similar blue-shift of the MLCT (metal-to-ligand charge-transfer) transition from 600 to 570 nm has been observed for bis(tetrabutylammonium)trithiocyanato(4,4′,4″-tricarboxy-2,2′:6′,2″-terpyridine)ruthenium(II) (known as black dye) by increasing the pH of the solution and is ascribed to deprotonation of the carboxylic acid group.[3]

Figure 2c shows absorption spectra of both dyes adsorbed on the surface of transparent 5 μm thick TiO_2 films. Absorption of the blank TiO_2 film was subtracted from the curve. Absorption spectra of both dyes were ~40−50 nm blue-shifted in the onset region when anchored at the TiO_2 surface compared to solution spectra. The stronger blue-shift of the CT-band of both dyes on TiO_2 films is attributed to π-stacking interactions or formation of aggregates on the TiO_2 surface. A blue-shift is commonly observed in the spectral response of organic

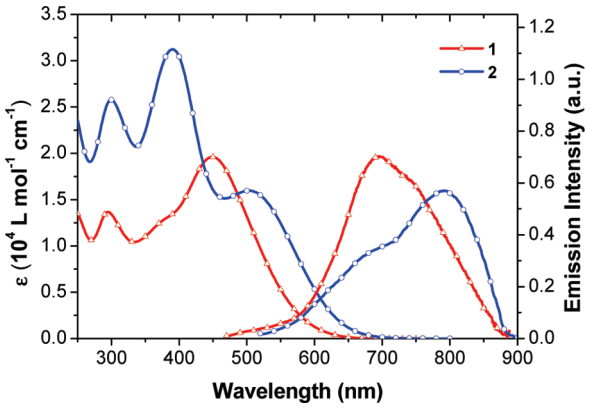

Figure 1. UV−vis and normalized emission spectra of dye **1** (red triangle) and **2** (blue circle) in dichloromethane. The emission spectra are normalized to their respective CT bands.

dyes adsorbed on the surface of TiO_2 compared to the solution, which is due to the electronic interactions of the dye to the semiconductor surface.[17] The concentration of the branched dye (0.11 M) adsorbed on the film is about half the concentration of the linear dye (0.23 M), which we attribute to impaired surface packing due to the large size of the branched molecule.

The observed CT character in solution was corroborated by semiempirical calculations. The quantum-chemical Austin Model 1 (AM1) method under restricted Harthree Fock conditions was used to analyze the electron distribution of the frontier orbitals of both dyes (Figure 3). The electron density distribution of the highest occupied molecular orbitals (HOMO) of both molecules is mainly located at the oligothiophene and diphenylamine moieties, whereas electron density of the lowest unoccupied molecular orbital (LUMO) is primarily located at the cyanoacrylic acid acceptor and the neighboring thiophene ring. Hence, the presence of strong electron density relocation between HOMO and LUMO is present and supports the occurrence of an intramolecular charge transfer transition (ICT) in the UV−vis spectra. Furthermore, the calculated electron distribution shows favorable directionality for injection of photoexcited electrons from the donor group to the TiO_2 film via the bridge and anchoring group.

Redox Properties. The energetic alignment of HOMO and LUMO energy levels is crucial for an efficient operation of the sensitizer in a DSSC. To ensure efficient electron injection from the excited dye into the conduction band of TiO_2 films, the LUMO level must be higher in energy than the TiO_2 conduction band edge. The HOMO level of the dye must be lower in energy than the redox potential of the I^-/I_3^- redox couple for efficient regeneration of the dye cation after photoinduced electron injection into the TiO_2 film. The electrochemical

(15) Mishra, A.; Ma, C.-Q.; Janssen, R. A. J.; Bäuerle, P. *Chem. Eur. J.* **2009**, *15*, 13521.

(16) Johansson, T.; Mammo, W.; Svensson, M.; Andersson, M. R.; Inganäs, O. *J. Mater. Chem.* **2003**, *13*, 1316.

(17) (a) Xu, M.; Wenger, S.; Bala, H.; Shi, D.; Li, R.; Zhou, Y.; Zakeeruddin, S. M.; Grätzel, M.; Wang, P. *J. Phys. Chem. C* **2009**, *113*, 2966. (b) Zhang, G.; Bai, Y.; Li, R.; Shi, D.; Wenger, S.; Zakeeruddin, S. M.; Grätzel, M.; Wang, P. *Energy Environ. Sci.* **2009**, *2*, 92.

Table 1. Optical and Electrochemical Data of Sensitizers L-3T-DPA 1 and B-5T-DPA 2 in Dichloromethane

dyes	λ^{ab} [nm] (ε [L mol^{-1} cm^{-1}])	$\lambda^{em}{}_{max}$ [nm]	$E_g{}^{opt}$ [eV]	$E^0{}_{ox1}$ [V] [b,c]	$E^0{}_{ox2}$ [V] [b,c]	HOMO [eV] [d]	LUMO [eV] [e]
L-3T-DPA (**1**)	295 (13700) 386 (13200)[a] 450 (19600)	694 737 (sh)	2.14	0.18	0.56	−5.19	−3.05
B-5T-DPA (**2**)	300 (25800) 390 (31200) 503 (16000)	680 (sh) 791	1.94	0.18	0.65	−5.19	−3.25

[a] Only visible as shoulder. [b] Measured in DCM/TBAHFP (0.1 M), $c \approx 1 \cdot 10^{-3}$ mol L^{-1}, 295 K, scan rate = 100 mV s^{-1}, vs Fc$^+$/Fc. [c] Values determined by cyclic voltammetry measurement. [d] Calculated from $E^{onset}{}_{ox1}$ set E_{HOMO}(Fc$^+$/Fc) = −5.1 eV vs vacuum.[16] [e] Determined from the optical band gap.

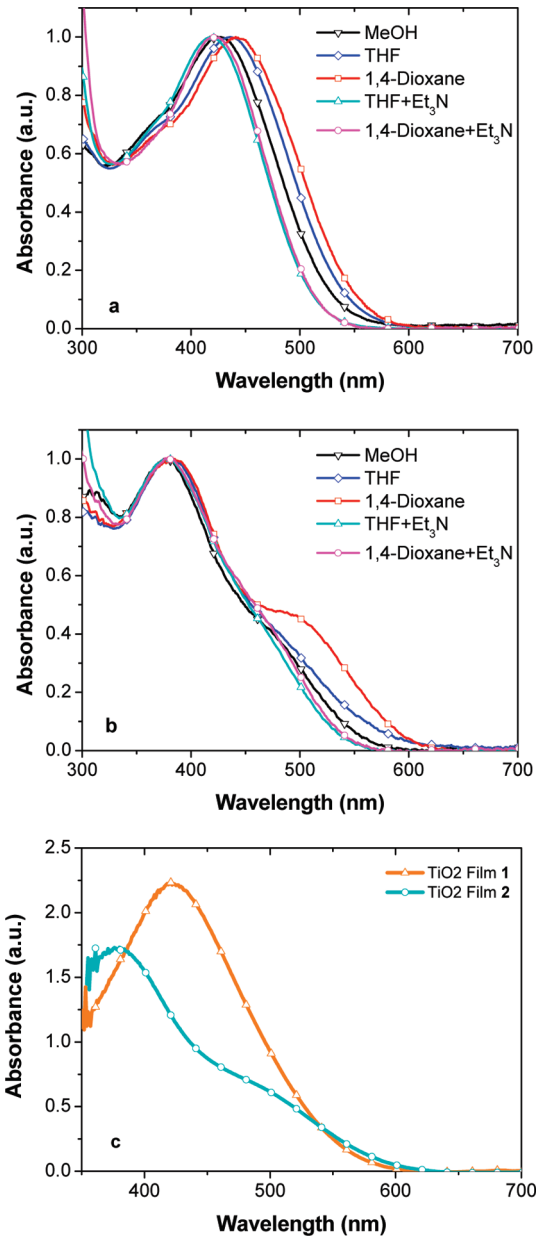

Figure 2. Normalized absorption spectra of (a) linear (**1**) and (b) branched (**2**) dye in different solvents. (c) Absorption spectra on transparent 5 μm thick TiO_2 films (blank TiO_2 film is subtracted from measurement).

behavior of the dyes was investigated by cyclic voltammetry, and the data are listed in Table 1. Reversible redox waves were obtained for both dyes in the oxidative region (Figure 4).

The first oxidation potential ($E^0{}_{ox1}$) for both compounds was found at 0.18 V (vs Fc$^+$/Fc) and is assigned to the oxidation of the diphenylthienyl-amine moiety.[18] The HOMO energy levels were calculated from the onset of the first oxidation wave ($E^{onset}{}_{ox1}$ = 0.09 V vs Fc/Fc$^+$) and resulted for both dyes to −5.19 eV. The second oxidation potential was observed at 0.56 and 0.65 V for **1** and **2**, respectively, and is assigned to the oxidation of the oligothiophene units. The LUMO levels of both sensitizers were calculated from the difference between HOMO energies and UV−vis absorption onset values. It is interesting to note that changing the donor from triphenylamine to diphenylthienyl-amine decreases the oxidation potential by about 290 mV, as the electron density is increased from phenyl to the more electron-rich thiophene.[9c]

The HOMO−LUMO levels of both dyes are suitable for DSSCs. The LUMO energy levels (**1**: −3.05 eV; **2**: −3.25 eV) are sufficiently higher than the conduction band edge of TiO_2 (−4.0 eV). Hence, an effective electron transfer from the excited dye to the TiO_2 is ensured. The HOMO energy levels of −5.19 eV for both dyes are about 360 meV lower in energy than the standard potential of the I_3^-/I^- redox couple (−4.83 eV vs vacuum),[7b] and thus a sufficient driving force for the regeneration of the oxidized dye is available.

Photovoltaic Performance and Device Stability. Photovoltaic tests were conducted to evaluate the potential of the linear and branched sensitizers in dye-sensitized solar cells (see the Experimental Section for detailed cell compositions). The incident photon-to-current conversion efficiencies (IPCE) of devices with dye **1** and **2** using an acetonitrile-based electrolyte are shown in Figure 5a. The IPCE of linear dye **1** exceeds 80% in the spectral region between 500 and 550 nm. Considering the light absorption and scattering loss by the conducting glass, the absorbed photon-to-current conversion efficiency (APCE) is close to unity in this region. In contrast, the IPCE of branched dye **2** has a maximum of 67% at 510 nm. The estimated maximum IPCE with dye **2**, assuming an APCE of unity, Lambert−Beer-type absorbance in the TiO_2 film, and accounting for reflectance and absorbance in the conducting glass, is about 10% higher than the measured IPCE. This loss is probably caused by reduced charge collection efficiency: The lower dye loading favors increased

(18) (a) Rohde, D.; Dunsch, L.; Tabet, A.; Hartmann, H.; Fabian, J. *J. Phys. Chem. B* **2006**, *110*, 8223. (b) Su, Y. Z.; Lin, J. T.; Tao, Y.-T.; Ko, C.-W.; Lin, S.-C.; Sun, S.-S. *Chem. Mater.* **2002**, *14*, 1884.

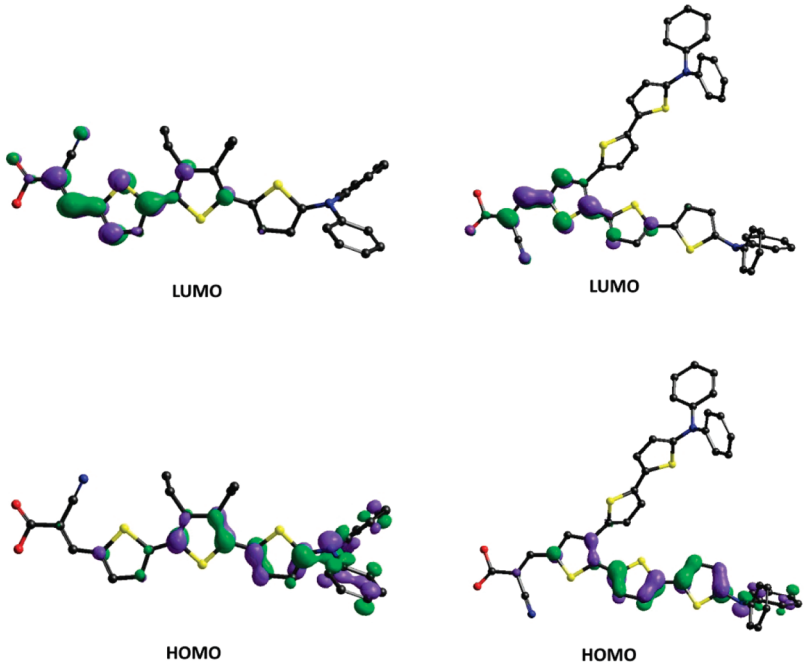

Figure 3. Frontier orbitals (AM1-calculation) of L-3T-DPA **1** (linear) and B-5T-DPA **2** (branched) (carbons in *black*, nitrogens in *blue*, oxygens in *red*, sulfurs in *yellow*, and hydrogens are omitted for clarity reasons).

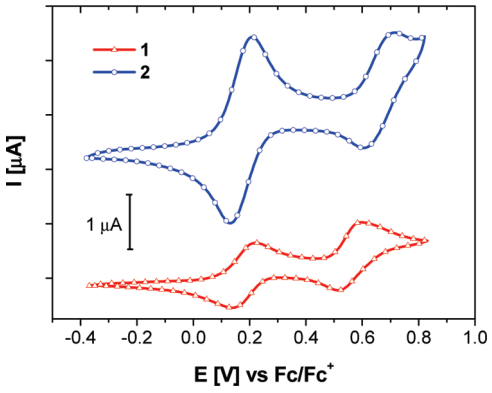

Figure 4. Cyclic voltammograms of **1** (red triangle) and **2** (blue circle); DCM/TBAHFP (0.1 M), $c \approx 1 \times 10^{-3}$ mol L^{-1}, 295 K, scan rate = 100 mV s^{-1}, vs Fc^{+}/Fc.

charge recombination between free electrons in the TiO_2 conduction band and oxidized species (tri-iodide) in the electrolyte at the uncovered TiO_2 surface. This hypothesis was confirmed with photovoltage decay experiments (see the section on Charge Recombination).

The photovoltaic parameters, i.e. conversion efficiency (η), short-circuit photocurrent density (J_{sc}), open-circuit photovoltage (V_{oc}), and fill factor (FF) under full sunlight (AM 1.5G, 100 mW cm^{-2}) of devices with volatile, ionic liquid electrolyte, and a solid hole conductor are summarized in Table 2. The photocurrent−voltage curves of the devices with volatile electrolyte are shown in Figure 5b. With the volatile electrolyte we measured a conversion efficiency of 6.8% for dye **1** and 5.0% for dye **2**. The lower J_{sc} of the device with branched dye **2** is consistent with the lower IPCE. The 40 mV lower V_{oc} can be explained with increased charge recombination via the exposed TiO_2 surface not covered with dye as discussed in more detail later. With the ionic liquid electrolyte, after 24 h of light soaking, we obtained stabilized values of 5.9% for dye **1** and 2.6% for dye **2**. The markedly lower photocurrent of branched dye **2** with ionic liquid electrolyte compared to volatile electrolyte is probably due to the large recombination current at the uncovered TiO_2 surface, since the ionic liquid electrolyte contains a high concentration of triiodide compared to the volatile electrolyte (about 0.24 M vs 0.03 M).[19] In solid-state devices with spiro-MeOTAD as a hole transporting material we measured efficiencies of 3.0% with dye **1** and 2.6% with dye **2** (Figure 6). Since it is difficult to fill the pores with the hole conductor, only thin films of TiO_2 (here 1.8 μm) can be used, which limit J_{sc} accordingly. However, V_{oc} is enhanced by about 200 mV since the redox level of the hole conductor is situated at a more negative energy (about −4.9 eV) than the redox level of the iodide/triiodide couple (about −4.83 eV). J_{sc} of the device with linear dye **1** is around 1.7 mA cm^{-2} higher than that with branched dye **2**. This result is consistent with the results of the liquid devices, where the adsorbed amount of dye **2** on the surface of TiO_2 is lower than for dye **1** resulting in lower J_{sc} values.

The stability of devices with ionic liquid electrolyte was tested over 1000 h at full sunlight and 60 °C. The evolution of the photovoltaic parameters is shown in Figure 7. The parameters were normalized to stabilized values after 24 h of light soaking, which allowed for optimal reorganization of the dye molecules on the TiO_2 surface. The cell with the linear dye **1** showed more rapid degradation of performance, retaining only 73% of its initial efficiency after 1000 h. We attribute this degradation to desorption of dye molecules, which induces a loss of J_{sc} and

(19) Bai, Y.; Cao, Y.; Zhang, J.; Wang, M.; Li, R.; Wang, P.; Zakeeruddin, S. M.; Grätzel, M. *Nat. Mater.* **2008**, *7*, 626.

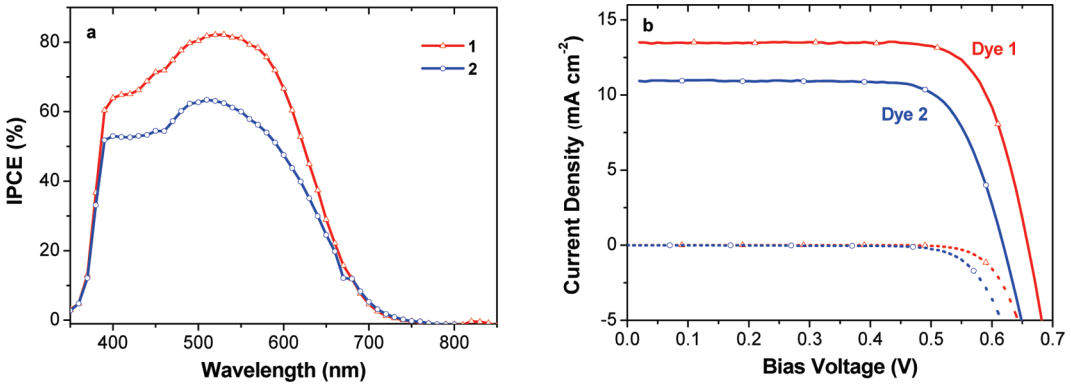

Figure 5. Incident photon-to-current conversion efficiency (a) and current density−voltage curve under full sunlight (AM 1.5G, 100 mW cm^{-2}) and in the dark (b) of devices sensitized with L-3T-DPA **1** (red triangle) and B-5T-DPA **2** (blue circle) using Z960 electrolyte.

Table 2. Photovoltaic Parameters of Devices with Sensitizers L-3T-DPA 1 and B-5T-DPA 2 in Liquid, Ionic Liquid, and Solid State DSCs at Full Sunlight (AM 1.5G, 100 mW cm^{-2})

dye	redox mediator	V_{oc} (mV)	J_{sc} (mA cm^{-2})	FF	η (%)
1 L-3T-DPA	volatile electrolyte (Z960)	659	−13.5	0.76	6.8
2 B-5T-DPA		619	−11.0	0.74	5.0
1 L-3T-DPA	ionic liquid (Z952)	659	−11.9	0.75	5.9
2 B-5T-DPA		570	−6.1	0.75	2.6
1 L-3T-DPA	solid hole conductor	834	−6.7	0.54	3.0
2 B-5T-DPA		827	−5.0	0.62	2.6

associated V_{oc}. In contrast, under similar conditions, the cell with branched dye **2** showed excellent photochemical and thermal stability, retaining 96% of its initial efficiency after 1000 h. The higher stability of the branched dye can be ascribed to two reasons: 1. the bulky structure of dye, which probably protect the TiO_2 surface and hinders desorption, and 2. suppression of electron transfer from TiO_2 to the electrolyte (i.e., dark current). This result means that the initial disadvantage of branched dye **2** is nearly ruled out.

Charge Recombination. We measured photovoltage decay transients of devices with the volatile electrolyte at various white light bias intensities in order to study charge recombination rates between electrons in the TiO_2 conduction band and tri-iodide ions in the electrolyte.[20] The recombination rates are plotted in Figure 8a versus the open-circuit potential (V_{oc}) of the device adjusted by varying the white light bias. Since V_{oc} in the device is given by the difference between the redox level of the electrolyte and the quasi-Fermi level of TiO_2, which is determined by the concentration of free charge carriers, this plot allows us to compare the recombination rate at equal charge density concentrations in the TiO_2 films. The recombination rate is known to increase exponentially with increasing bias light due to a filling of intraband trap states in the TiO_2, which allows a faster detrapping of electrons to the conduction band and subsequent recombination with tri-iodide.[21] We measured an approximate 4-fold increase in recombination rate for the device with branched dye **2**

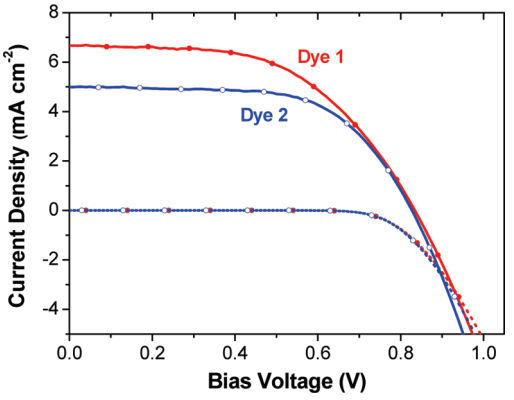

Figure 6. Current density−voltage curve under full sunlight (AM 1.5G, 100 mW cm^{-2}) and in the dark of devices sensitized with L-3T-DPA **1** and B-5T-DPA **2** using a solid hole conductor. TiO_2 film thickness 1.8 μm, overnight dipping, 0.4 cm^2 active surface area.

compared to linear dye **1**, which we attribute to an increased recombination current via the larger fraction of uncovered TiO_2 surface. The chemical capacitance of the TiO_2/electrolyte interface in devices with dye **1** or **2** is plotted vs V_{oc} in Figure 8b. The chemical capacitance is proportional to the density of trap states (DOS) at the quasi-Fermi level corresponding to that V_{oc} and commonly shows an exponential distribution.[22] We found a lateral shift to the left of about 25 mV of the DOS curve of the device with dye **2**. This shift is most likely due to a change in the surface charge on the uncovered TiO_2 surface, i.e. a positive charging by free protons in the electrolyte, which induces a downward shift of the conduction band of the TiO_2 toward the iodide/tri-iodide potential. Both the higher recombination rate and the downward shifted conduction band in the device with dye **2** explain the lower V_{oc} measured in the current−voltage curves. Additionally, the higher charge recombination rate reduces the charge collection efficiency and consequently the J_{sc} and IPCE.

Conclusion

We have synthesized two D-π-A organic dyes comprising linear and branched oligothiophenes for application

(20) Duffy, N. W.; Peter, L. M.; Wijayantha, K. G. U. *Electrochem. Commun.* **2000**, *2*, 262.
(21) Bisquert, J.; Vikhrenko, V. S. *J. Phys. Chem. B* **2004**, *108*, 2313.
(22) Bisquert, J. *Phys. Chem. Chem. Phys.* **2003**, *5*, 5360.

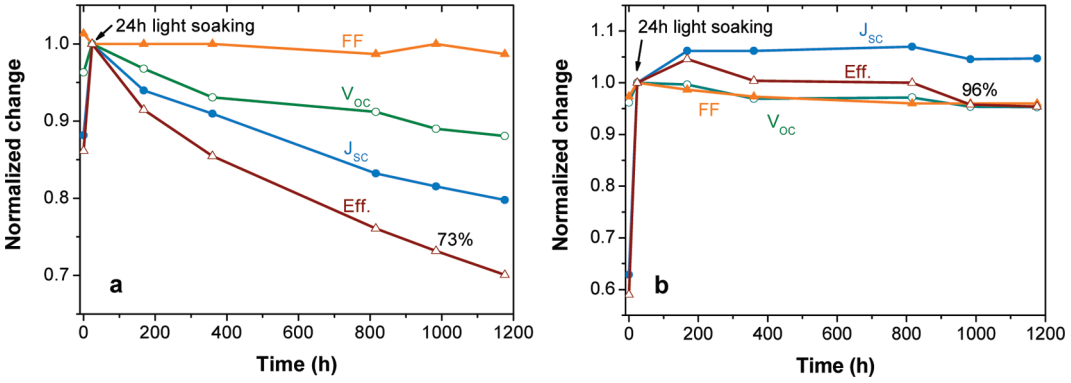

Figure 7. Photovoltaic parameters of devices using the linear dye **1** (a) and the branched dye **2** (b) during a 1000 h accelerated stability test (full sunlight, 60 °C). Parameters are normalized to stabilized values after 24 h of light soaking.

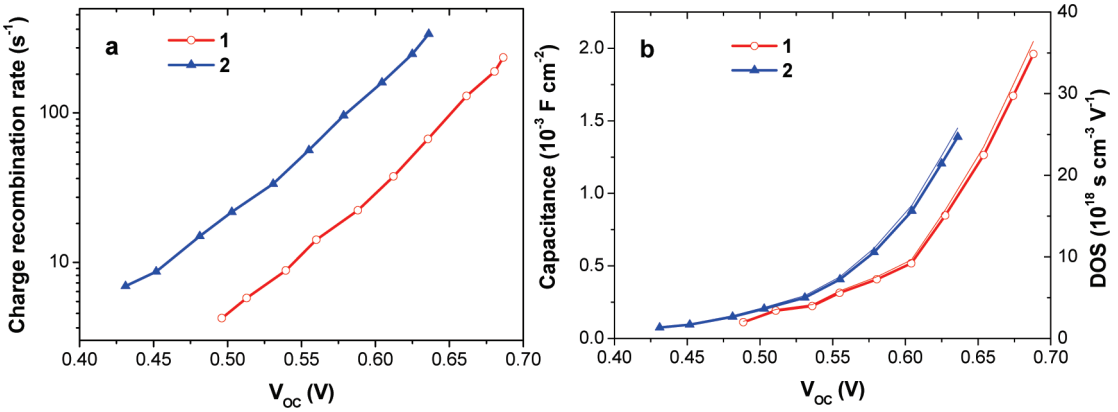

Figure 8. Comparison of (a) charge recombination kinetics and (b) chemical capacitance and density of trap states (DOS) of dye **1** (red) and **2** (blue) in devices with the branched and linear dye.

in dye-sensitized solar cells. In a nonvolatile electrolyte, IPCE of the linear dye **1** exceeding 80% in the spectral region between 500 and 550 nm was observed with an overall conversion efficiency of 6.8%. The lower efficiency in the case of branched dye **2** is ascribed to the reduction of the photocurrent due to less dye loading on the TiO_2 surface. A moderate decrease in the efficiency was observed for the linear dye in ionic liquid devices, whereas for the branched dye the efficiency was reduced to half. The performance of both dyes in solid-state devices is nearly similar. An approximate 4-fold increase in the recombination rate was measured for the device with branched dye **2** compared to linear dye **1** in volatile electrolyte, which was attributed to an increased recombination current via the larger fraction of uncovered TiO_2 surface. Long-term stability measurements of devices with ionic liquid electrolyte were performed over 1000 h at full sunlight and 60 °C showing higher stability for the cell comprising branched dye. This result shows that the initial disadvantage of branched dye **2** is nearly ruled out. The higher durability of the branched dye makes this molecular design an interesting option in further development of new molecules, where compromise on the dye loading should be minimized.

Acknowledgment. We thank Pascal Comte for TiO_2 film preparation and Carole Grätzel for fruitful discussions. S.W., M.W., S.M.Z., and M.G. thank the Swiss National Science Foundation for financial support and A.M, M.K.R.F, and P.B thank the German Ministry of Education and Research (BMBF) for financial support in the frame of project OPEG 2010.